

Sphaleron and gravitational wave with the Higgs-Dilaton potential in the Standard Model Two-Time Physics

Vo Quoc Phong^{a,b,*}, Quach Ai Mi^{a,b,†} and Nguyen Xuan Vinh^{a,b,‡}

^a*Department of Theoretical Physics, University of Science, Ho Chi Minh City 700000, Vietnam*

^b*Vietnam National University, Ho Chi Minh City 700000, Vietnam*

By introducing a Higgs-Dilaton potential, the 2T model has a trigger for a first order electroweak phase transition, namely for the mass of Dilaton between 300 GeV and 550 GeV. We have also compared the transition strengths in the case with and without daisy loops, the difference being always less than 0.2. The effective Higgs potential has given a sphaleron energy less than 8.4 TeV. The timescale of phase transition (β/H^*) is larger than 25 and less than 34 in all cases that are sufficient to trigger the first order electroweak phase transition. Gravitational wave energy density caused by this transition, may be detected by future detectors, could indirectly confirm Dilaton.

Keywords: Spontaneous breaking of gauge symmetries, Extensions of electroweak Higgs sector, Particle-theory models (Early Universe)

I. INTRODUCTION

Multidimensional theories have become an important phenomenological research framework. However, from 2008, besides the string theory, the multi-dimensional model that fully combines with particle physics is currently only the 2T theory [1–7]. The one not only provides us with a new view of time but also suggests new explanations for difficult problems such as the matter-antimatter asymmetry and the strong-CP problem. The cause of them may be from an exotic particle in the 2T model, Dilaton.

The 2T model is a form of space-time extension but at the same time proposes a new

*Electronic address: vqphong@hcmus.edu.vn

†Electronic address: aimiwu14498@gmail.com

‡Electronic address: vinhnguyen.mxt@gmail.com

particle, Dilaton which is originally a dark matter candidate. However, the role of Dilaton could be more numerous. It as previously investigated is a source of strong CP violation and is likely also responsible for the matter-antimatter asymmetry.

The first order electroweak phase transition (EWPT) problem was solved in the 2T elementary particle model. According to current research, the triggers can be Dark matter (DM) or new heavy bosons Refs. [8–34]. As in the studies of other authors, the cause of first order phase transition is due to the dominant activation of Dilaton which is stored in an external potential of Dilaton.

Dilaton is a common name. The concept of Dilaton also appears in many other theories such as the composite Higgs models. However, Dilaton in the 2T model is a particle associated with the concept of two time dimensions and the symmetry $SP(2, R)$.

At present, the evidence for extra dimensions is very weak. Instead of looking for it, the 2T model needs to be enabled and look for the evidence of Dilaton. This also indirectly proves the existence of extra dimensions. The electroweak phase transition may be the clue for this search. Because the problem can give us the possible mass domain of Dilaton, sketching a form of Dilaton potential. In addition, it makes clearer the mass generation scenario for particles.

In Ref.[35], we proposed a form of Dilaton potential with the non-zero mass Dilaton which is sufficient to trigger a first order electroweak phase transition. However, in Ref.[35] with a one-loop effective potential without daisy loops, the necessary mass domain for Dilaton is given but not completely. In this paper, an effective potential with daisy loops is used to recalculate more accurately the phase transition strength (S) and other quantities in the Baryogenesis scenario. Specifically the sphaleron energy and the gravitational wave energy (GW) density are calculated.

This article is organized as follows. In section II, the types of Dilaton potentials are discussed. Then the strength of EWPT is calculated in the case of a one-loop effective potential with Daisy loops. The comparison of phase transition strength in the case with and without daisy loops. In section III, by using static fields and spherically symmetric bubble nucleations, sphaleron energy and gravitational waves are solved numerically with a wide range of Dilaton mass. We make a general assessment of sphaleron energies, comparing the gravitational wave energy density with current data. Finally, we summarize and make outlooks in section IV, such as evaluating the compatibility of sphaleron with other conditions

and giving a way to search for an first order electroweak phase transition.

II. CONTROLLING EWPT BY THE HIGGS-DILATON POTENTIAL

The basic concepts as well as the 2T elementary particle model of 2T theory were built by I. Bars [5] when considering multidimensional concepts. In our opinion, it is like an extension of the concept of time. This model has successes such as solving the problem of strong CP violation, providing DM candidates [3].

The SM in the 2T model includes the Higgs scalar fields H and Dilaton Φ , the left/right chiral fermion fields Ψ^L, Ψ^R (which are quarks and leptons), and the gauge bosons A_M that accompany the gauge symmetry of this model [5].

With the $SP(2, R)$ symmetry, the Higgs-Dilaton potential [6] has the following form,

$$V(\Phi, H) = \lambda (H^\dagger H - \alpha^2 \Phi^2)^2 + V(\Phi), \quad (1)$$

in which λ, α are dimensionless couplings. The Dilaton Φ and the Higgs doublet H which are the $SO(4, 2)$ scalar fields [5],

$$\Phi = (1, 1)_0, \quad H = \begin{pmatrix} H^+ \\ H^0 \end{pmatrix}_{\frac{1}{2}} = (1, 2)_{\frac{1}{2}}.$$

Initially $V(\Phi)$ had no specific form. But it is the key to examining EWPT and related quantities [36]. The minimization process Eq. (1) leads to the Higgs and Dilaton fields having non-zero VEV and being proportional to each other [5, 35].

After reducing to 1T [5, 37], we get the 4D Higgs-Dilaton potential as follows:

$$V(h, \phi) = \lambda [\chi^2 - \alpha^2 \phi^2]^2 + V(\phi), \quad \chi(x) = \frac{1}{\sqrt{2}}(v + h(x)), \quad \phi = \frac{1}{\alpha\sqrt{2}}(v + \alpha d(x)), \quad (2)$$

in which $v = 246$ GeV, h, d scalar fields with zero VEVs. When $v(\phi)$ is involved, h, d are not physical fields yet. Because $V(h, \phi)$ will contain mixed components between h and d . Depending on the form of $V(\Phi)$, the diagonalization process will yield physical particles.

Because of the $SP(2, R)$ symmetry, in 6-dimensional spacetime, the potential of scalar field must have a form of fourth powers of field. Therefore, the Dilaton potential is rewritten in its general form as $f(\mathcal{S}/\Phi) \cdot \Phi^4$, from which we see that the potential must always be the even power of field. The Dilaton field in the 2T model with a potential of only fourth power, is like a degree of freedom or it has near zero mass but has a non-zero VEV.

So this is something different from SM. However, the electroweak symmetry breaking is accompanied by the $SP(2, R)$ symmetry breaking. When this symmetry is broken, the Dilaton potential is no longer only of fourth power. This can be explained mathematically by choosing the function $f(\mathcal{S}/\Phi)$.

The form of $V(\Phi)$ is still under consideration in some cases, for example in connection with gravity. In Table I the choices of $V(\Phi)$ are summarized.

$f(\mathcal{S}/\Phi)$	$V(H, \Phi)$	\mathcal{S}	$V(\Phi)$	Refs.
$V(H, \Phi) = f(\mathcal{S}/\Phi)\Phi^4$				
$\frac{\lambda}{4}(\mathcal{S}^2/\Phi^2 - \alpha^2)^2 + \rho/4$	$\lambda (H^\dagger H - \alpha^2 \Phi^2)^2 + \rho \Phi^4$	$\sqrt{2H^\dagger H}$	$\rho \Phi^4$	Refs.[36]
$\frac{\lambda}{4}(\mathcal{S}^2/\Phi^2 - \alpha^2)^2 + \rho/4 + \frac{\omega^2}{\kappa^2 \Phi^2}$	$\lambda (H^\dagger H - \alpha^2 \Phi^2)^2 + \rho \Phi^4 + \frac{\omega^2}{\kappa^2} \Phi^2$	$\sqrt{2H^\dagger H}$	$\rho \Phi^4 + \frac{\omega^2}{\kappa^2} \Phi^2$	Refs.[35, 36]

TABLE I: Cases of the Higgs-Dilaton potential

A. The Dilaton potential

In this study, an added Dilaton potential has the following form [35]:

$$V(\Phi) = \rho \Phi^4 - \frac{\omega^2}{\kappa^2} \Phi^2. \quad (3)$$

ω is much smaller than κ . ω has the mass dimension, κ is the scaling constant when reducing from the 2T to 1T spacetime, κ is a mixture of the extra dimension and the second time dimension so it has the length dimension [5, 36]. The second power component of field in Eq.3 is a soft-breaking component of the $SP(2, R)$ symmetry. It implies the second power component of field, $\frac{\omega^2}{\kappa^2} \phi^2$ is very small compared to the fourth power component. As in Ref.[35], $V(\Phi) \sim \text{const.} \Phi^4 + \text{const.} \Phi^2$ has been assumed. In general, we can choose κ to be arbitrarily large, so the above inequality can always be satisfied. After reducing from 2T to 1T, the potential will be in the form,

$$V(\phi) = \frac{\rho}{\kappa^4} \phi^4 - \frac{\omega^2}{\kappa^4} \phi^2. \quad (4)$$

Therefore we introduce only even-order components of the Dilaton field. This assumption could be justified if one takes into account the next leading order of 2T metric in the action

[5] and Z_2 symmetry of Dilaton. κ^4 will be simplified by the 2T action when reduced to 1T [5]. Then by substituting the above Higgs and Dilaton fields into the Higgs-Dilaton potential, the potential is rewritten in terms of the variable ϕ_c which is a re-notation of VEV,

$$\begin{aligned} V(h, \phi) &= \frac{\lambda}{4} [(\phi_c + h)^2 - (\phi_c + \alpha d)^2]^2 - \frac{\omega^2}{2\alpha^2}(\phi_c + \alpha d)^2 + \frac{\rho}{4\alpha^4}(\phi_c + \alpha d)^4 \\ &= \left\{ \left(\frac{\rho}{4\alpha^4}\phi_c^4 - \frac{\omega^2}{2\alpha^2}\phi_c^2 \right) + \left(\frac{\rho}{\alpha^3}\phi_c^3 - \frac{\omega^2}{\alpha}\phi_c \right) d \right. \\ &\quad \left. - 2\lambda\alpha\phi_c^2hd + \lambda\phi_c^2h^2 + \left(\lambda\alpha^2\phi_c^2 - \frac{\omega^2}{2} + \frac{3\rho}{2\alpha^2}\phi_c^2 \right) d^2 \right\} + \text{interaction terms}, \end{aligned} \quad (5)$$

Eq.(5) appears the term hd so they are not physical particles yet. In the 2T spacetime, the $\omega^2/\kappa^2\Phi^2$ component will be so small that it can be neglected. However, when reducing the spacetime to 1T, the κ^4 parameter in Eq.(4) is lost, so the $\omega^2\phi^2$ component can have a significant contribution and lead to a Dilaton with non-zero mass.

The diagonalization process requires that the components proportional to the field d must cancel. Therefore $\left(\frac{\rho}{\alpha^3}\phi_c^3 - \frac{\omega^2}{\alpha}\phi_c \right) = 0$, which leads to $\omega^2 = \frac{\rho}{\alpha^2}\phi_c^2$. This relation can not hold in the first order phase transition. It changes with ϕ_c . However, the mathematical form is not likely to be preserved in the electroweak phase transition. This is similar to how some authors have modified the Yukawa interaction which leads to a first order electroweak phase transition (as shown in Ref.[38]). But in the simplest of considerations, we assume that this form does not change. This is similar to considering that the mathematical form of the masses of particles may not change. But in the basic sense, this form can be considered unchanged. If we change this form, the interaction between the Higgs and the Dilaton will change very strongly, which requires the assumption of some other mechanism.

After diagonalization, we obtain physical particles which have masses at tree level as [35]

$$\begin{aligned} m_{d'}^2 &= \frac{2\alpha^4\lambda\phi_c^2 + 2\alpha^2\lambda\phi_c^2 + 3\rho\phi_c^2 - \alpha^2\omega^2}{2\alpha^2} \\ &\quad - \frac{\sqrt{8\alpha^2\lambda\phi_c^2[\alpha^2\omega^2 - 3\rho\phi_c^2] + [\phi_c^2(2\alpha^4\lambda + 2\alpha^2\lambda + 3\rho) - \alpha^2\omega^2]^2}}{2\alpha^2}, \end{aligned} \quad (6)$$

$$\begin{aligned} m_{h'}^2 &= \frac{2\alpha^4\lambda\phi_c^2 + 2\alpha^2\lambda\phi_c^2 - \alpha^2\omega^2 + 3\rho\phi_c^2}{2\alpha^2} \\ &\quad + \frac{\sqrt{8\alpha^2\lambda\phi_c^2[\alpha^2\omega^2 - 3\rho\phi_c^2] + [\phi_c^2(2\alpha^4\lambda + 2\alpha^2\lambda + 3\rho) - \alpha^2\omega^2]^2}}{2\alpha^2}. \end{aligned} \quad (7)$$

In Eq. (6), as ω and ρ go to zero, $m_{d'}^2 = 0$, which is in agreement with the results in Ref. [5]. The above formulas can be rewritten as follows

$$m_{h'}^2(\phi_c) = A\phi_c^2; m_{d'}^2(\phi_c) = B\phi_c^2, \quad (8)$$

here A, B are the parameteres. As ϕ_c approaches 0, $m_{d'}$ and $m_{h'}$ actually approach 0 in Eqs. (6) and (7). According to the approximation formulas (Eqs. (8)), when $\phi_c \rightarrow 0$, $m_{d'} \rightarrow 0$ and $m_{h'} \rightarrow 0$.

For convenience, h', d' will be denoted again as \mathcal{H}, \mathcal{D} in the following sections. The contribution of extra dimensions does not only appear in one effective potential via Dilaton but also in the mass of Higgs and other fields as well.

Thus, Dilaton has a very interesting property, the manifestation of Dilaton in 1T space-time is a massless particle. Or in other words, the manifestation of 6-dimensional spacetime (2T spacetime) is through the mass of Dilaton.

Furthermore, from the 2T sectors reduced to 1T, analyzed and diagonalized, the masses of top quark and gauge fields are obtained [3, 5], respectively,

$$m_t^2(\phi_c) = \frac{h_t^2}{2}\phi_c^2 = \frac{m_t^2}{v^2}\phi_c^2, \quad (9)$$

$$m_W^2(\phi_c) = \frac{g_1^2}{4}\phi_c^2 = \frac{m_W^2}{v^2}\phi_c^2, \quad (10)$$

$$m_Z^2(\phi_c) = \frac{g_1^2 + g_2^2}{4}\phi_c^2 = \frac{m_Z^2}{v^2}\phi_c^2, \quad (11)$$

where $m_i \equiv m_i(v)$ is the mass of field i at the zero temperature and $v = 246$ GeV, is equal to the VEV of Higgs in SM. As the temperature drops to zero, the VEV of the Higgs field increases to 246 GeV. Here ϕ_c is understood as VEV at temperature T . Therefore, the change from the symbol v to ϕ_c in the previous steps is convenient for writing expressions at temperature T . From Eq.(8) to Eq.(11), the full mass spectra of particles that make significant contributions to the effective potential.

B. The effective potential and searching S

The mass generation mechanism for particles in this model is still through the Higgs field like SM, however the Higgs field is always accompanied by the Dilaton field since the creation of non-zero VEV of the Higgs field requires a Dilaton field. This process is clearly shown in the minimization of the Higgs-Dilaton potential [2–7, 35].

The effective one-loop potential is usually calculated in the manner of Jackiw [39–41] which is developed from the Coleman-Weinberg potential. The effective one-loop potential at 0K can be written as

$$V_{\text{eff}}^{0K}(\phi_c) = \frac{\lambda_R}{4}\phi_c^4 - \frac{m_R^2}{2}\phi_c^2 + \Lambda_R + \frac{1}{64\pi^2} \sum_{i=\mathcal{H},\mathcal{D},W,Z,t} n_i m_i^4(\phi_c) \ln \frac{m_i^2(\phi_c)}{v^2},$$

where $\lambda_R, m_R, \Lambda_R$ are renormalized parameters, $m_i(\phi_c)$ is mass at tree level derived in previous subsection, i.e., SM particles and Dilaton; n_i with $i = \mathcal{D}, \mathcal{H}, W, Z, t$ are constants related to the degrees of freedom of each field and are given by

$$n_{\mathcal{H}} = n_{\mathcal{D}} = 1, n_W = 6, n_Z = 3, n_t = -12.$$

To work out renormalized parameters, we have dropped the constant Λ_R , which results in the effective potential at 0 being 0, hence $V_{\text{eff}}(v) = V_{\text{eff}}(0) = 0$. The familiar normalization conditions will be used,

$$\begin{cases} V_{\text{eff}}(v) = V_{\text{eff}}(0) = 0, \\ V'_{\text{eff}}(v) = 0, \\ V''_{\text{eff}}(v) = m_{\mathcal{H}}^2, \end{cases}$$

from which the coefficients in the effective potential are found out the following results

$$\begin{cases} \lambda_R = \frac{m_{\mathcal{H}}^2}{2v^2} - \frac{1}{16\pi^2 v^4} \sum_i n_i m_i^4 \left(\ln \frac{m_i^2}{v^2} + \frac{3}{2} \right), \\ m_R^2 = \frac{m_{\mathcal{H}}^2}{2} - \frac{1}{16\pi^2 v^2} \sum_i n_i m_i^4, \\ \Lambda_R = \frac{m_{\mathcal{H}}^2 v^2}{8} - \frac{1}{128\pi^2} \sum_i n_i m_i^4. \end{cases}$$

Another problem arises, the small value of ϕ_c/T_c causes the perturbation theory to break down due to infrared divergence at high temperatures and only non-perturbative calculations are acceptable. To solve this divergence problem we will add second order divergent daisy loops, that is, add n second order divergent loops as shown in Figure 1.

In case the daisy loops are taken into account, at the high temperature, the effective potential takes the form,

$$V_{\text{eff}}(\phi_c, T) = \frac{\lambda(T)}{4}\phi_c^4 + D(T^2 - T_0^2)\phi_c^2 - \frac{T}{12\pi} \sum_{\mathcal{H},W,Z,\mathcal{D}} g_i \left[\frac{m_i^2(v)\phi_c^2}{v^2} + \Pi_i(T) \right]^{\frac{3}{2}}. \quad (12)$$

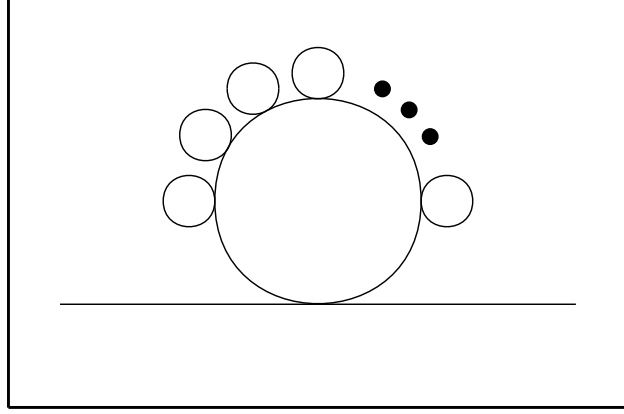


FIG. 1: Contribution of n -loop daisy to the self-energy for the scalar field.

If we do not consider daisy loops, Eq.(12) will not have Π_i functions, the coefficients in Eq.(12) are of the form,

$$\lambda(T) = \frac{m_{\mathcal{H}}^2}{2v^2} + \frac{1}{16\pi^2 v^4} \left(\sum_{i=\mathcal{H},\mathcal{D},W,Z} n_i m_i^4 \ln \frac{A_b T^2}{m_i^2} + n_t m_t^4 \ln \frac{A_f T^2}{m_t^2} \right),$$

$$D = \frac{m_{\mathcal{H}}^2 + m_{\mathcal{D}}^2 + 6m_W^2 + 3m_Z^2 + 6m_t^2}{24v^2},$$

$$T_0^2 = \frac{1}{D} \left[\frac{m_{\mathcal{H}}^2}{4} - \frac{1}{32\pi^2 v^2} \sum_{i=\mathcal{H},\mathcal{D},W,Z,t} n_i m_i^4 \right].$$
(13)

The contributions of daisy loops are stored in the following functions,

$$\Pi_W(T) = \frac{22}{3} \frac{m_W^2}{v^2} T^2, \quad (14)$$

$$\Pi_Z(T) = \frac{22}{3} \frac{(m_Z^2 - m_W^2)}{v^2} T^2, \quad (15)$$

$$\Pi_h(T) = \frac{m_{\mathcal{H}}^2 + 2m_W^2 + m_Z^2 + 2m_t^2}{4v^2} T^2, \quad (16)$$

$$\Pi_d(T) \sim \frac{m_{\mathcal{D}}^2}{v^2} T^2. \quad (17)$$

In Eq.(12), $\ln A_b = 3.907$ or $\ln A_f = 1.135$, and there is an additional contribution of Dilaton, which will push the EWPT process to be more intense. As analyzed in the case without daisy loops in Ref.[35], $300 \text{ GeV} \leq m_{\mathcal{D}} \leq 650 \text{ GeV}$, it will have the large enough EWPT strength (S). However, when the mass of Dilaton is too large, it will lead to large error in the effective potential. In Ref.[35] only S is calculated but the convergence conditions and errors of the effective potential are not taken into account. The first we can see this, if the ratio between mass and temperature (m/T) is not less than 2.2 the potential difference

will be in error by more than 5% [42]. The second, in Table II, when the Dilaton mass is larger than 550 GeV, ϕ_c does not converge to 246 GeV but exceeds 246 GeV.

$S = \frac{\phi_c}{T_c}$, is the ratio of VEV to the temperature at the time of phase transition. T_c is called the critical temperature. With the equations from Eq.(12) to Eq.(16), we can probe S for any given mass of Dilaton. The daisy loop contribution of Dilaton is ignored because its mass is larger than that of Top quark and at temperatures around 100 – 200 GeV its contribution is small. Also the exact calculation of these contributions is quite complicated, we can only estimate them as Eq.(17). The equations from (14) to (16), can be found in Refs.[43–45] for details, reduces the value of 3rd order component in Eq.(12), leading to S decreasing when there are daisy loops.

In Table II, S with daisy loops is always smaller than one without daisy loops. However, this difference does not exceed 0.2 or 10%. This also further confirms that the contribution of daisy loops in the critical temperature region is negligible but their contributions become significant in the higher one.

In summary, the first order EWPT has been recalculated in this section and then calculate the sphaleron energy and gravitational wave in the next section. The steps to find S are as follows:

- Choosing the Dilaton mass domain. Following Ref.[35], we choose the Dilaton mass from 300 GeV. Running the effective potential for different temperatures. T_c is the temperature for which $v_{eff}(\phi_c, T_c) = 0$.
- ϕ_c is the second non-zero VEV of v_{eff} . From there we calculate $S = \frac{\phi_c}{T_c}$. The convergence condition for ϕ_c is that it must be less than 246 GeV.

$m_{\mathcal{D}}$ [GeV]	v_c [GeV]	T_c [GeV]	S	E_{sph}^T [GeV]	E_0 [GeV]	α	$\frac{\beta}{H^*}$	$\Omega h^2(f_{peak})$	Daisy loops
300	107.492	136.162	0.789439	7658.14	9106.11	0.00766406	25.3093	6.34889×10^{-16}	without
	98.2028	146.281	0.671331	7636.04		0.00480408	23.4906	1.08379×10^{-16}	with
350	133.417	129.726	1.02845	7751.48	9094.9	0.0132065	26.8886	5.07648×10^{-15}	without
	128.617	138.449	0.928987	7727.12		0.00945377	25.1155	1.46259×10^{-15}	with
400	160.455	122.702	1.30768	7905.02	9079.14	0.0211503	28.991	2.958×10^{-14}	without
	158.371	130.329	1.21517	7888.4		0.0161664	27.2371	1.10564×10^{-14}	with
450	190.502	115.103	1.65505	8113.7	9055.43	0.0326829	31.7208	1.44943×10^{-13}	without
	189.376	121.835	1.55436	8106.3		0.0256766	29.9408	6.06993×10^{-14}	with
500	229.877	108.027	2.12796	8392.06	9020.63	0.0522199	34.9581	7.77137×10^{-13}	without
	227.515	113.854	1.99831	8384.29		0.0410284	33.1385	3.30201×10^{-13}	with
550	287.102	106.276	2.70147	8792.76	8970.03	0.0938256	37.2308	6.25938×10^{-12}	without
	281.168	110.832	2.53687	8769.76		0.0725315	35.6069	2.57741×10^{-12}	with
600	348.246	114.415	3.04372	9264.72	8895.83	0.158098	36.4387	3.90875×10^{-11}	without
	339.772	117.85	2.88309	9229		0.123424	35.2402	1.73786×10^{-11}	with

TABLE II: Results in the cases of Dilaton.

III. SPHALERON AND GRAVITATIONAL WAVE

Under the conditions of Sakarov [9], B violation must be mandatory and requires the existence of a sufficiently large sphaleron rate or sphaleron are relevant for the B violating processes.

The sphaleron energy functional consists of three components: the contribution of gauge fields, the Higgs kinetic energy and the effective potential.

$$E_{sph} = \int dx^3 \left[\frac{1}{4} W_{ij}^a W_{ij}^a + (D_i \phi)^\dagger (D_i \phi) + V_{eff} \right]. \quad (18)$$

With the static field approximation (ie., $W_0^a = 0$) and sphaleron in the spherically sym-

metric form [46]:

$$\begin{cases} \phi(r) = \frac{v}{\sqrt{2}} h(r) i n_a \sigma^a \begin{pmatrix} 0 \\ 1 \end{pmatrix}, \\ W_i^a(r) = \frac{2}{g} \epsilon^{aij} n_j \frac{f(r)}{r}, \end{cases} \quad (19)$$

where $n_i \equiv \frac{x^i}{r}$ and r is the radial coordinate in the spherical coordinates. σ^a are the Pauli matrices and $a = 1, 2, 3$. ϵ^{ij} is the Levi-Civita symbol.

The non-zero temperature Sphaleron energy functional is written as follows

$$E_{sph}^T = \frac{4\pi v}{g} \int_0^\infty d\xi \left[4 \left(\frac{df}{\xi} \right)^2 + \frac{8f^2(1-f)^2}{\xi^2} + \frac{\xi^2}{2} \left(\frac{dh}{\xi} \right)^2 + h^2(1-f)^2 + \frac{\xi^2}{g^2 v^4} V_{eff}(h, T) \right], \quad (20)$$

in which $g^2 = \frac{G_F 8m_W^2}{\sqrt{2}}$; $G_F = 1.166 \times 10^{-5} \text{ GeV}^{-2}$; $m_W = 80.39 \text{ GeV}$, $\xi \equiv gvr$.

Taking the variation of above function in terms of $h(\xi)$ and $f(\xi)$, we will obtain the equations of motion,

$$\xi^2 \frac{d^2 f}{d\xi^2} = 2f(1-f)(1-2f) - \frac{\xi^2}{4} h^2(1-f), \quad (21)$$

$$\frac{d}{d\xi} \left(\xi^2 \frac{dh}{d\xi} \right) = 2h(1-f)^2 + \frac{\xi^2}{g^2 v^4} \frac{\partial V_{eff}}{\partial h}. \quad (22)$$

The contribution of effective potential to the sphaleron energy is less than 45%, but the effective potential acts as a source for bubbles (as seen from Eq.(21) and (22)).

Here, $h(\xi)$ and $f(\xi)$ have boundary conditions

$$\begin{cases} h(\xi \rightarrow 0) = f(\xi \rightarrow 0) = 0, \\ h(\xi \rightarrow \infty) = f(\xi \rightarrow \infty) = 1. \end{cases} \quad (23)$$

These boundary conditions ensure that the sphaleron energy converges, because from Eqs. (22), (21) and (20), as ξ increases, the functions $f(\xi)$, $h(\xi)$ must approach 1 and the components in Eq.(20) must approach 0. For equations from (20) to (23), the numerical solutions are obtained as Figs. 2, 3, 4, 5 and Table II.

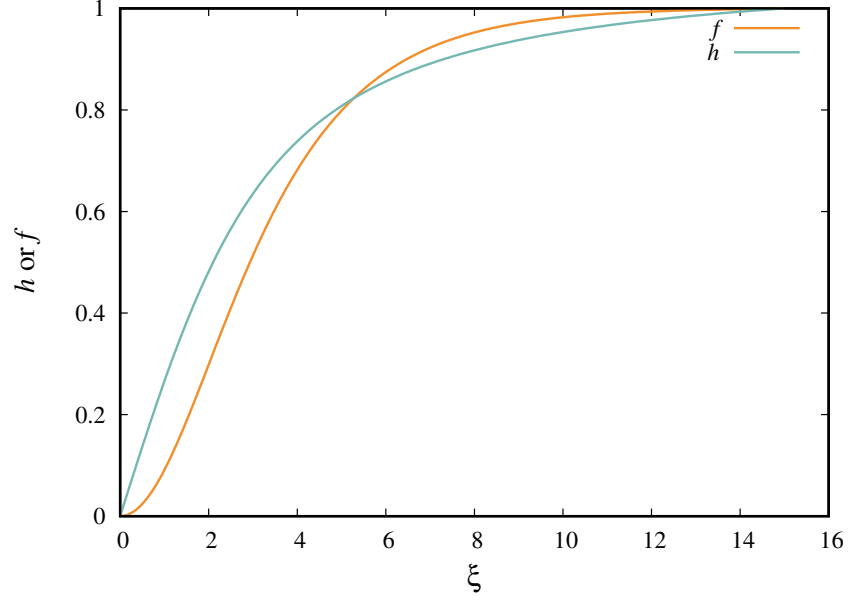


FIG. 2: Profile functions with $m_{\mathcal{D}} = 300$ GeV.

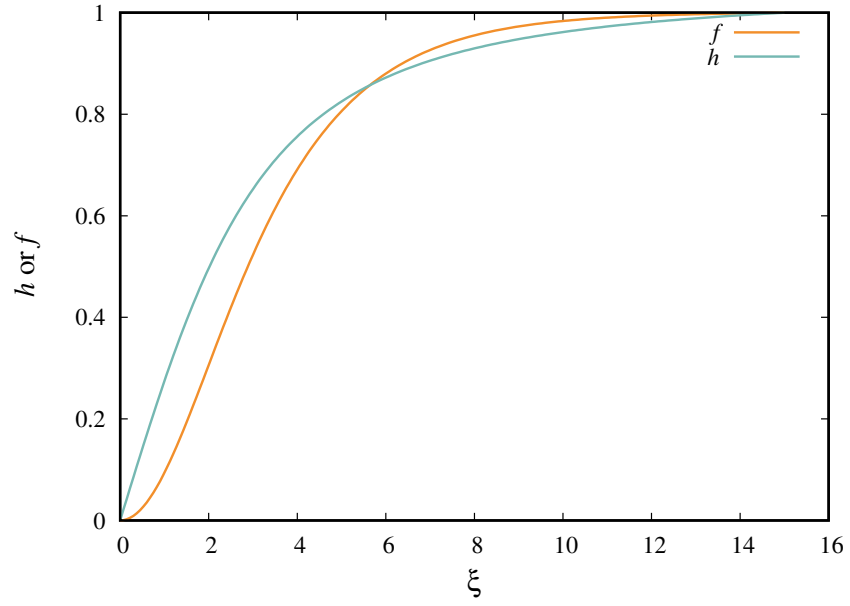
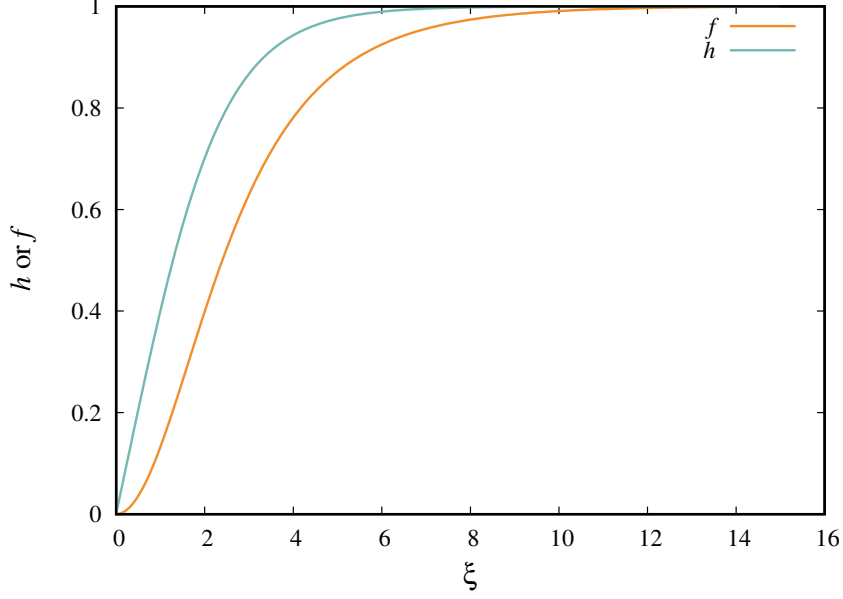
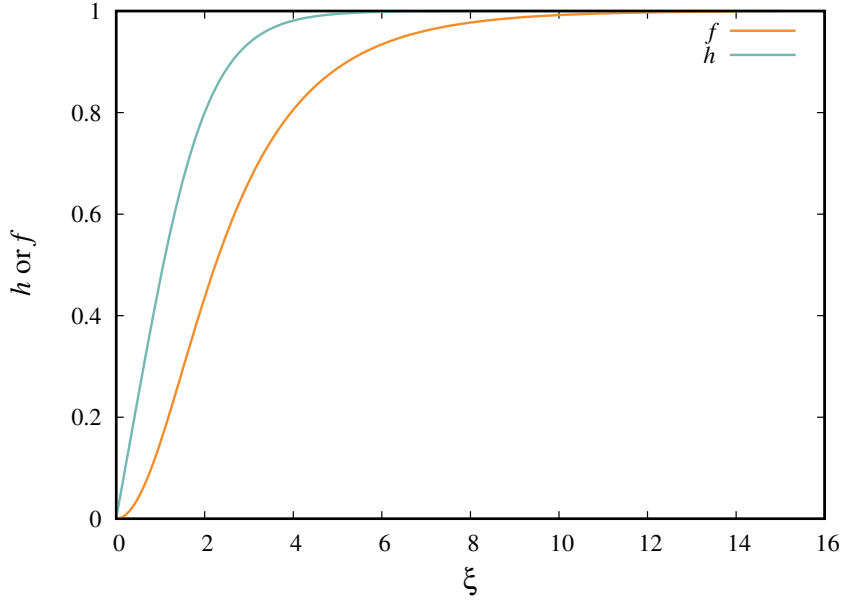


FIG. 3: Profile functions with $m_{\mathcal{D}} = 350$ GeV.

FIG. 4: Profile functions with $m_{\mathcal{D}} = 550$ GeV.FIG. 5: Profile functions with $m_{\mathcal{D}} = 600$ GeV.

In Figs. 2-5, the larger the mass of Dilaton is, the faster $f(\xi), h(\xi)$ approaches 1. This is consistent with the results in Table II, the larger the mass of Dilaton is, the larger S is. When $m_{\mathcal{D}} < 350$ GeV, $f(\xi)$ approaches 1 faster than $h(\xi)$ but when $m_{\mathcal{D}} > 350$ GeV this approach to 1 happens in reverse. Because the larger m_d is, the stronger the interaction between Higgs and Dilaton is, further delaying the expansion of Higgs bubble nucleation.

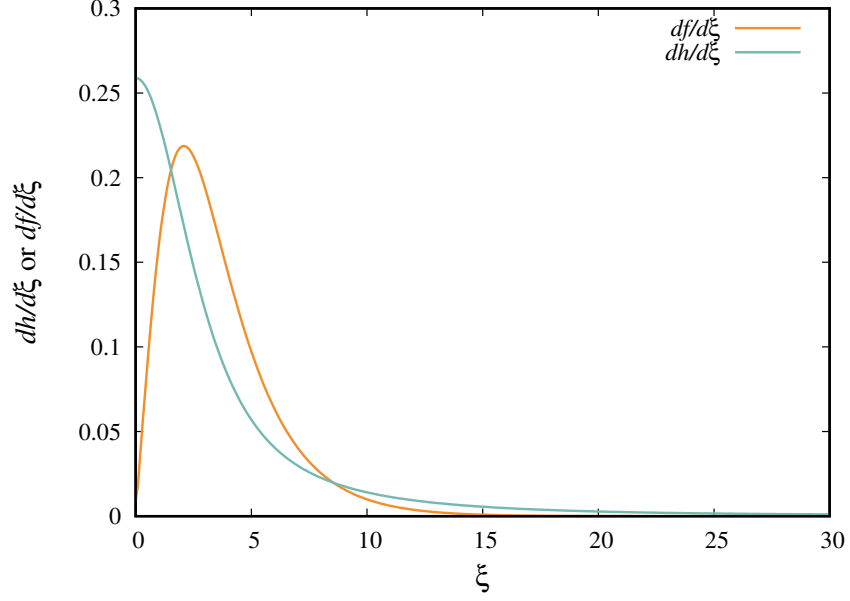


FIG. 6: $dh/d\xi$ and $df/d\xi$ with $m_D = 300$ GeV.

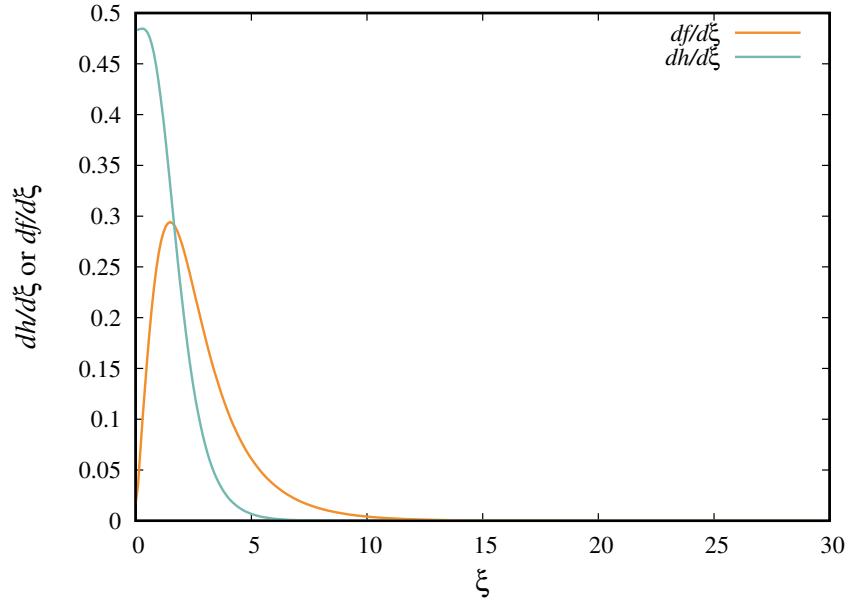


FIG. 7: $dh/d\xi$ and $df/d\xi$ with $m_D = 600$ GeV.

Figs.6 and 7 show the expansion speed of bubbles (like the bounces of bubbles) corresponding to the solutions in Figs.2 and 5. $dh/d\xi$ always decreases as ξ increases. $df/d\xi$ increases to a maximum value and then also decreases as ξ increases. Additionally, this numerical calculation can also be done by referring to the packages in Ref.[47].

The largest sphaleron energy is about 9.2 TeV with the Dialton mass of about 600 GeV. But to avoid the VEV divergence problem, the Dilaton mass must be less than 550 GeV, therefore the sphaleron energy in this model is about 8.4 TeV. This energy range is about 1 TeV smaller than that in the SM.

There are three processes which are involved in the production of GWs at a first-order PT: Collisions of bubble walls, sound waves in the plasma and Magnetohydrodynamic (MHD) turbulence [48]. These three processes generically coexist, and the corresponding contributions to the stochastic GW background should linearly combine, at least approximately, so that [48]

$$h^2\Omega_{GW} = h^2\Omega_{Coll} + h^2\Omega_{sw} + h^2\Omega_{tur}. \quad (24)$$

The first parameter α is determined at the nucleation temperature as follows [49–51]:

$$\alpha = \frac{\epsilon}{\rho_{rad}^*}, \quad (25)$$

$$\epsilon = \left(V_{eff}(v(T), T) - T \frac{d}{dT} V_{eff}(v(T), T) \right)_{T=T_C}, \quad (26)$$

$$\rho_{rad}^* = g^* \pi^2 \frac{T_c^4}{30} = 106.75 \pi^2 \frac{T_c^4}{30}. \quad (27)$$

This parameter depends only on the configuration of effective potential. Thus in all models the parameter which is easily calculated by usual way when the effective potential is known, determines the strength of phase transition.

There are three different scenarios depending on the bubble wall velocity [48] which is defined via α :

$$v_b = \frac{\frac{1}{\sqrt{3}} + \sqrt{\alpha^2 + \frac{2\alpha}{3}}}{1 + \alpha}. \quad (28)$$

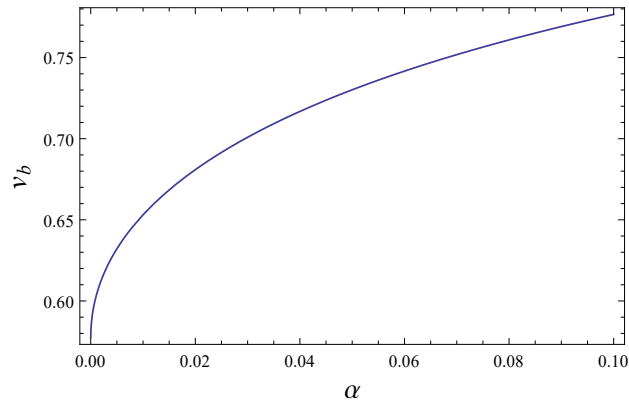


FIG. 8: The behavior of v_b depends on α .

With the values of α in Table II, $0.009 < \alpha < 0.16$ and Fig.8 represents Eq. 28. Comparison between Table II and Fig.8, we see that $v_b \approx 0.65 - 0.75$. It is not much smaller than 1 so that we approximate $v_b \sim 1$. If $v_b \ll 1$, we must have other approximations about Ωh^2 [48]. Therefore, the generation of gravitational waves has only two components: the sound wave and turbulence [48, 52–57]. The gravitational wave energy density parameters of sound waves is defined as follows [48, 58]:

$$h^2 \Omega_{sw}^2(f) = 2.65 \cdot 10^{-6} v_b k_w^2 \frac{H^*}{\beta} \left(\frac{\alpha}{1+\alpha} \right)^2 \left(\frac{100}{106.75} \right)^{1/3} S_{sw}(f), \quad (29)$$

where

$$\begin{cases} S_{sw} = \left(\frac{f}{f_{peak,sw}} \right)^3 \left(\frac{7}{4+3\left(\frac{f}{f_{peak,sw}}\right)^2} \right)^{7/2} \\ v_b \sim 1. \\ k_w = \alpha(0.73 + 0.083\sqrt{\alpha} + \alpha)^{-1}. \end{cases} \quad (30)$$

And GWs from turbulence in the cosmic fluid is given by

$$h^2 \Omega_{tur}^2(f) = 3.35 \cdot 10^{-4} \left(\frac{k_t \alpha}{1+\alpha} \right)^{3/2} \frac{H^*}{\beta} \left(\frac{100}{106.75} \right)^{1/3} S_{tur}(f), \quad (31)$$

in which

$$\begin{cases} S_{tur} = \left(\frac{f}{f_{peak,tur}} \right)^3 \left(\frac{1}{1+\left(\frac{f}{f_{peak,tur}}\right)} \right)^{11/3} \frac{1}{1+8\pi f/h^*} \\ H^* = \frac{16.5 \cdot 10^{-3} T_c}{100} \left(\frac{106.75}{100} \right)^{1/6}; v_b \sim 1. \\ k_t = 0.05\alpha(0.73 + 0.083\sqrt{\alpha} + \alpha)^{-1}. \\ f_{peak,tur} = 2.7 \cdot 10^{-2} \frac{\beta}{H^*} \frac{T_c}{100} \left(\frac{106.75}{100} \right)^{1/6}. \end{cases} \quad (32)$$

$f_{peak,sw/tur}$ are the frequencies at which Ωh^2 reaches maxima. Because the effective potential contributes about 45% to the sphaleron energy. We have a possible approximation [37] for the second parameter (the timescale of phase transition),

$$\frac{\beta}{H^*} \approx \left[T \frac{d(S(t))}{dT} \right]_{T=T_N} \approx \left[T \frac{d(S_3/T)}{dT} \right]_{T=T_N} \approx \left[T \frac{d\left(0.45 \frac{E_{sph}^T}{T}\right)}{dT} \right]_{T=T_N}. \quad (33)$$

T_N in Eq. (33) is a nucleation temperature which is usually smaller than T_c . Although at T_c , S_3 diverges [59], the sphaleron energy can be determined. Therefore, we need to determine a nucleation temperature T_N and then calculate $\frac{\beta}{H^*}$. Instead, we try to approximate

S_3 with the sphaleron energy. To avoid supercooling, T_N should not be too much larger than T_c or the supercooling parameter $\delta_{sc,n} = \frac{T_c - T_N}{T_c}$ [59] must not be too big. Also because determining the nucleation temperature is quite cumbersome but it is negligibly smaller than T_c , so we use T_c in the third approximation step in Eq.(33).

The third approximation in Eq.(33) is due to the fact that S_3 does not contain components of the gauge fields. In Table III, the Higgs contribution (E_{Higgs}^T is the component that contains only the h function in Eq.(20)) to the total sphaleron energy is estimated to be about 45%.

The third approximation in Eq.(33) is an imperfect approximation. It is just an estimate for determining $\frac{\beta}{H^*}$. Usually the value of this quantity is fixed at around 10 – 100 [48, 59] for calculating gravitational waves. Therefore the estimates in the third approximation also give acceptable values (specifically from 25 to 37, as in Table II). Also when we have calculated the sphaleron energy, Eq.(33) is a convenient approximation or we are just trying to change the context from determining the pair (T_N, S_3) to the pair (T_c, E) . This is a mathematical technique but it requires physical care.

$m_{\mathcal{D}}[GeV]$	With daisy loops			Without daisy loops		
	$E_{Higgs}^{T_c}[GeV]$	$E_{sph}^{T_c}[GeV]$	$E_{Higgs}^{T_c}/E_{sph}^{T_c}(\%)$	$E_{Higgs}^{T_c}[GeV]$	$E_{sph}^{T_c}[GeV]$	$E_{Higgs}^{T_c}/E_{sph}^{T_c}(\%)$
400	3691.73	7889.04	46.7957	3695.42	7905.67	46.7439
450	3740.08	8107.09	46.1334	3741.64	8114.49	46.1106
500	3805.29	8385.24	45.3809	3807.15	8393.02	45.3609
550	3910.02	8770.95	44.5793	3916.76	8793.96	44.5392
600	4058.26	9230.51	43.9657	4070.84	9266.26	43.9319
650	4213.12	9640.4	43.7027	4228.75	9678.84	43.6907
700	4354.95	9971.64	43.6734	4371.84	10008.8	43.6798

TABLE III: The ratio between the Higgs component and the total sphaleron energy.

The contribution of daisy loops to the effective potential is negligible. Therefore, in this section, we will use the effective potential without the daisy loops to calculate the sphaleron and gravitational wave energies. From equations (29), (31) and related formulas, we solve numerically and obtain the results at $T_N \approx T_c$ in Table II and Figs. 9, 10. From Table II, the sphaleron energies with and without daisy loop do not differ much.

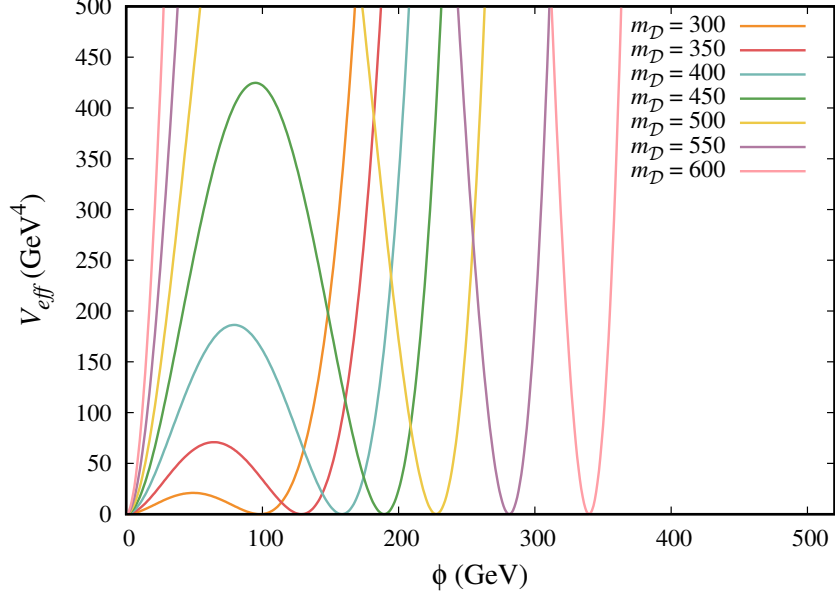


FIG. 9: The effective potential with $m_{\mathcal{D}} = 300 - 600$ GeV.

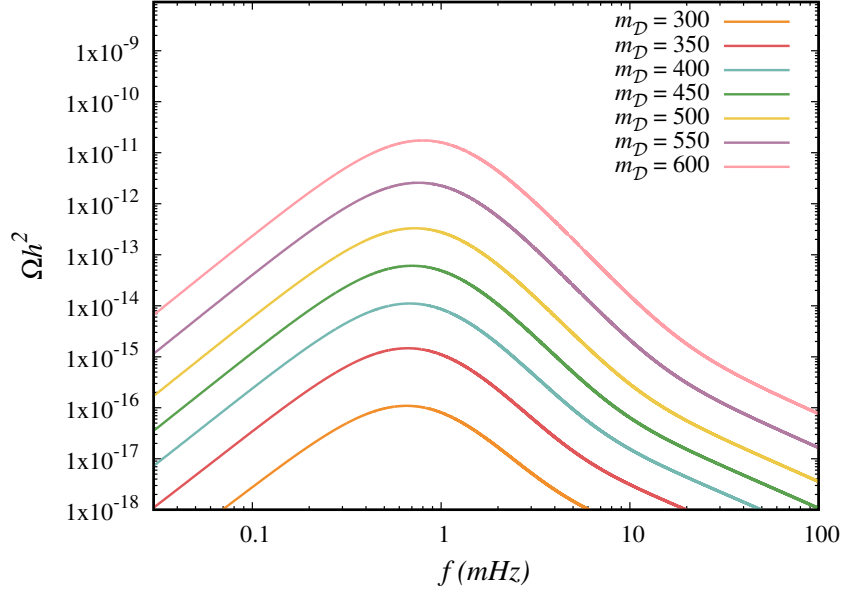


FIG. 10: Gravitational wave energy density with $m_{\mathcal{D}} = 300 - 600$ GeV.

When the mass of Dilaton changes, the effective potential also changes so the sphaleron energy will change leading to Ωh^2 depending on $m_{\mathcal{D}}$. In Fig.10, the larger $m_{\mathcal{D}}$ is, the higher the barrier of effective potential is, the higher the maximum of Ωh^2 is. Because the higher the barrier is, the more violent the EWPT process is, so the gravitational waves generated from it are larger. In Fig. 10, for $300 \text{ GeV} \leq m_{\mathcal{D}} < 600 \text{ GeV}$, the maximum value of Ωh^2 lies

in the range from 10^{-16} to 10^{-11} . This is a very wide range, or in other words Ωh^2 increases very rapidly over a mass range of 300 GeV. Furthermore, for Ωh^2 to increase 10 times, the mass of Dilaton increases by 50 GeV.

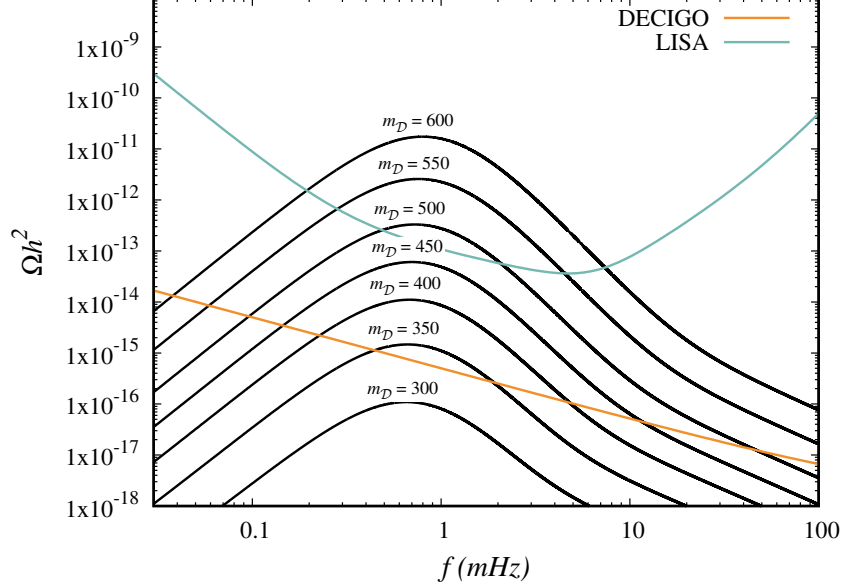


FIG. 11: With out the daisy loops, $m_{\mathcal{D}} = 300 - 600$ GeV, gravitational wave energy density compared with the LISA and DECIGO data.

TABLE IV: Sensitivity of proposed GW

$f[mHz]$	Ωh^2	Observatory	Ref.
0.02 – 0.12	$[0.02 - 1] \times 10^{-10}$	LISA	Refs.[60–62]
	$[0.5 - 8] \times 10^{-14}$	DECIGO	Refs.[60–62]
	—	BBO	Refs.[60–62]

The region from 10^{-14} to 10^{-11} is quite important, corresponding to $400 \text{ GeV} \leq m_{\mathcal{D}} < 550 \text{ GeV}$, because it can be included in the residual sensitivities of the experiment. Specifically, based on sensitivity data of future detector, in Table IV, LISA and DECIGO can pick up the signal of gravitational waves generated by the EWPT process in this model as shown in Fig. 11. Furthermore, as long as $m_{\mathcal{D}} < 500 \text{ GeV}$, gravitational waves from EWPT can be detected. The frequency domain for the maximum gravitational wave energy densities are 0.4–1.2 mHz which lies within the detection range of LISA, DECIGO and BBO.

In Table II, we have calculated that $\frac{\beta}{H_*} = \left[T^{\frac{d(0.45 \frac{E_{sph}^T}{T})}{dT}} \right]_{T=T_N}$ has values from 25 to 35 at temperatures from 120 to 140 GeV and $\gamma = \left[T^{\frac{d(S_3/T)}{dT}} \right]_{T=T_N}$ has values from 27 to 40. We find the difference between γ and $\frac{\beta}{H_*}$ to be in the range of 10% to 20%. But the difference value still gives a value of Ωh^2 within the detection range of LISA and DECIGO.

IV. CONCLUSION AND DISCUSSION

The electroweak phase transition is triggered by the Dilaton to be of first order. The sphaleron energy and the gravitational wave energy density are calculated and shown to be compatible with future experimental sensitivities. Furthermore, the results in the article also indicate that the contributions of the daisy loops to the sphaleron energy are negligible.

$m_{\mathcal{D}}$ [GeV]	v_c [GeV]	T_c [GeV]	S	E_{sph}^T [GeV]	E_0 [GeV]	E_0/v_0	E_c/v_c	$\frac{ E_0/v_0 - E_c/v_c }{E_0/v_0}$	Decoupling	Daisy loops
300	107.492	136.162	0.789	7658.14	9106.11	37.01	71.24	92.48%	57.09	without
	98.2028	146.281	0.671	7636.04			77.75	110%	53.57	with
350	133.417	129.726	1.028	7751.48	9094.9	36.98	58.1	57.11%	59.78	without
	128.617	138.449	0.928	7727.12			60.07	62.43%	56.17	with
400	160.455	122.702	1.307	7905.02	9079.14	36.91	49.26	33.45%	63.69	without
	158.371	130.329	1.215	7888.4			49.8	34.92%	60.04	with
450	190.502	115.103	1.655	8113.7	9055.43	36.81	42.59	15.7%	69.02	without
	189.376	121.835	1.554	8106.3			42.8	16.27%	65.27	with
500	229.877	108.027	2.127	8392.06	9020.63	36.67	36.5	0.4%	75.42	without
	227.515	113.854	1.998	8384.29			36.85	0.49%	71.59	with
550	287.102	106.276	2.701	8792.76	8970.03	36.46	30.61	16%	79.74	without
	281.168	110.832	2.536	8769.76			31.19	14.45%	76.34	with
600	348.246	114.415	3.043	9264.72	8895.83	36.16	26.6	26.43%	77.64	without
	339.772	117.85	2.883	9229			27.16	24.89%	75.16	with

TABLE V: Results with the decoupling condition and the scaling law.

The sphaleron scaling law [63–65], is assumed to calculate the sphaleron energy at high temperatures when it is known at 0K (E_0 or $E(0K)$). It assumes that $E(0K) = \frac{v}{v_T}E(T)$. However, as the data in Table IV, this law is not exact. Because $v_{eff}(0k)$ and $v_{eff}(T)$ are discontinuous when $T \rightarrow 0$. $v_{eff}(T)$ is only valid for $T \neq 0$. This law can only be true in the temperature range from T_N (the nucleation one) to T_c . Furthermore, from Table IV, E_0 decreases very slowly, $E(T)$ increases rapidly corresponding to $300 \text{ GeV} \leq m_D \leq 600 \text{ GeV}$. Because $f(\xi), h(\xi)$ at 0K approach 1 more slowly than they do at a non-zero temperature. However, this law is accurate for $m_D = 400 \text{ GeV}$ which may be the best value for Dilaton.

The decoupling condition [66–68], the important one, which is related to the sphaleron rate and the expansion rate of Universe,

$$\frac{E_{sph}(T)}{T} - 7\ln\left(\frac{v(T)}{T}\right) + \ln\left(\frac{T}{100\text{GeV}}\right) > 43. \quad (34)$$

In Table IV, the sphaleron energy at T_c fully satisfies the condition in Eq.(34). Although the right-hand side of Eq.(34) may be slightly changed, the values in the 10th column of Table IV are considerably larger than 43.

In the future, LISA, DECIGO and BBO can detect gravitational waves in the expected range. The GW of EWPT calculations could be a hint to indicate that there may be a contribution from the EWPT process in the detected wave spectrum. Additionally, the gravitational wave observations relevant to the early universe are summarized in Ref.[69]. Thus we have completely investigated the EWPT problem, calculating the Sphaleron energy and gravitational waves.

The calculation of $\frac{\beta}{H^*}$ is only an estimate. If the mass of Dilaton is determined from other data channels, we will calculate T_N and S_3 accurately and re-determine this parameter. This is an interesting future work for us.

In the 2T model, Dilaton is initially introduced to construct the 2T standard model through the $SP(2, R)$ symmetry, then we continue to analyze the role of Dilaton in the EWPT problem. The standard model is added with a scalar singlet, it will be very difficult for us to explain or explain why we need to add a singlet (but there are many models built from the standard model with a scalar singlet). Thus, in terms of the dynamics of the EWPT problem, Dilaton in the 2T model is similar to a scalar singlet that is added in the standard model. However, in a larger context (i.e., in conjunction with Cosmology), Dilaton in the 2T model is directly connected to the 6-dimensional spacetime. In other words, the EWPT

problem is explained by Dilaton in the 2T model, leaving us open that extra dimensions may exist. This is something that a pure scalar singlet fails to address.

ACKNOWLEDGMENTS

This research is funded by University of Science, VNU-HCM under grant number T2024-10.

-
- [1] I. Bars, C. Deliduman and D. Mimic, Phys. Rev. D **59**, 125004 (1999).
 - [2] I. Bars, Phys. Rev. D **62**, 046007 (2000).
 - [3] I. Bars, AIP conference proceedings **607**, 17 (2002).
 - [4] I. Bars, Class. and Quantum Grav. **18**, 3113-3130 (2001).
 - [5] I. Bars, Phys. Rev. D **74**, 085019 (2006).
 - [6] I. Bars and Y-C. Kuo, Phys. Rev. D **74** 085020 (2006).
 - [7] I. Bars , Phys.Rev.D **74**, 085019 (2006).
 - [8] G. W. Anderson and L. J. Hall, Phys. Rev. D **45**, 2685-2698 (1992).
 - [9] A. D. Sakharov, JETP Lett.**5**, 24 (1967).
 - [10] M. Bastero-Gil, C. Hugonie, S. F. King, D. P. Roy, and S. Vempati, Phys. Lett. B **489**, 359 (2000).
 - [11] A. Menon, D. E. Morrissey, and C. E. M. Wagner, Phys. Rev. D **70**, 035005 (2004).
 - [12] S. W. Ham, S. K. Oh, C. M. Kim, E. J. Yoo, and D. Son, Phys. Rev. D **70**, 075001 (2004).
 - [13] J. M. Cline, G. Laporte, H. Yamashita, S. Kraml, JHEP **0907**, 040 (2009).
 - [14] S. Kanemura, Y. Okada, E. Senaha, Phys. Lett. B **606**, 361-366 (2005).
 - [15] G. C. Dorsch, S. J. Huber, J. M. No, JHEP **10**, 029 (2013).
 - [16] S. W. Ham, S-A Shim, and S. K. Oh, Phys. Rev. D **81**, 055015 (2010).
 - [17] V. Q. Phong, V. T. Van, and H. N. Long, Phys. Rev. D **88**, 096009 (2013).
 - [18] V. Q. Phong, H. N. Long, V. T. Van, N. C. Thanh, Phys. Rev. D **90**, 085019 (2014).
 - [19] V. Q. Phong, H. N. Long, V. T. Van, L. H. Minh, Eur. Phys. J. C **75**, 342 (2015).
 - [20] J. Sá Borges, R. O.Ramos, Eur. Phys. J. C **76**, 344 (2016).
 - [21] S. Kanemura, E. Senaha, T. Shindou and T. Yamada, JHEP **1305**, 066 (2013).

- [22] D. J. H. Chung and A. J. Long, Phys. Rev. D **81**, 123531 (2010) .
- [23] G. Barenboim and N. Rius, Phys. Rev. D **58**, 065010 (1998).
- [24] F. Pisano and V. Pleitez, Phys. Rev. D **46**, 410 (1992).
- [25] P. H. Frampton, Phys. Rev. Lett. **69**, 2889 (1992).
- [26] R. Foot *et al*, Phys. Rev. D **47**, 4158 (1993).
- [27] M. Singer, J. W. F. Valle and J. Schechter, Phys.Rev. D **22**, 738 (1980).
- [28] R. Foot, H. N. Long and Tuan A.Tran, Phys. Rev. D **50**, R34 (1994).
- [29] J. C. Montero, F. Pisano and V. Pleitez, Phys. Rev. D **47**, 2918 (1993).
- [30] H. N. Long, Phys. Rev. D **54**, 4691 (1996).
- [31] H. N. Long, Phys. Rev. D **53**, 437 (1996).
- [32] A. J. Buras, F. De Fazio, J. Girrbach and M. V. Carlucci, JHEP **1302**, 023 (2013).
- [33] H. H. Patel, M. J. Ramsey-Musolf, JHEP **1107**, 029 (2011).
- [34] G. W. Anderson and L. J. Hall, Phys. Rev. D **45**, 2685 (1992).
- [35] Vo Quoc Phong and Dam Quang Nam, International Journal of Modern Physics A, Vol. 38, Nos. 29 & 30 (2023) 2350159.
- [36] I. Bars, P. Steinhardt, Neil Turok, Phys.Rev.D **89**, 043515 (2014).
- [37] Vo Quoc Phong, Nguyen Chi Thao, and Hoang Ngoc Long, Eur. Phys. J. C **82**, 1005 (2022).
- [38] I. Baldes, T. Konstandin, and G. Servant, Phys.Lett.B **786**, 373 (2018).
- [39] S. Coleman and E. Weiberg, Phys. Rev. D **7**, 1888 (1973).
- [40] R. Jackiw, Phys. Rev. D **9**, 1686 (1974).
- [41] L. Dolan and R. Jackiw, Phys. Rev. D **9**, 3320 (1974).
- [42] G. W. Anderson and L. J. Hall, Phys. Rev. D **45**, 2685 (1992).
- [43] M. E. Carrington, Phys. Rev. D **45**, 2933 (1992).
- [44] David Curtin, Patrick Meade, Harikrishnan Ramani, Eur. Phys. J. C **78**, 787 (2018).
- [45] A. Katz and M. Perelstein, JHEP **07** 108 (2014).
- [46] Xucheng Gan, Andrew J. Long, and Lian-Tao Wang, Phys. Rev. D **96**, 115018 (2017).
- [47] C.L. Wainwright, Comput. Phys. Commun. **183**, 2006 (2012).
- [48] Chiara Caprini, etc. , JCAP**04**, 001 (2016).
- [49] L. Leita, A. Megevand, A. D. Sanchez, JCAP **10**, 024 (2012).
- [50] M. S Tuner and S. Wilzek, Phy. Rev. **65**, 3080 (1990).
- [51] Christophe Grojean, G. Servant, Phys. Rev. D **75**, 043507 (2007).

- [52] A. Kosowsky, M. S. Turner, and R. Watkins, Phys. Rev. D **45**, 4514 (1992).
- [53] A. Kosowsky, M. S. Turner, and R. Watkins, Phys. Rev. Lett. **69**, 2026 (1992).
- [54] A. Kosowsky and M. S. Turner, Phys. Rev. D **47**, 4372 (1993).
- [55] S. J. Huber and T. Konstandin, JCAP **08099**, 022 (2008).
- [56] R. Jinno and M. Takimoto, Phys. Rev. D **95**, 024009 (2017).
- [57] R. Jinno and M. Takimoto, JCAP **1901**, 060 (2019).
- [58] R. Zhou, L. Bian and H-K Guo, Phys. Rev. D **101**, 091903 (2020).
- [59] Peter Athron, Csaba Balázs, Lachlan Morris, JCAP **03**, 006 (2023).
- [60] S.V. Demidov, D. S. Gorbunov, D. V. Kirpichnikov, Physics Letters B **779**, 191 (2018).
- [61] Hideaki Kudoh, Atsushi Taruya, Takashi Hiramatsu, and Yoshiaki Himemoto, Phys. Rev. D **73**, 064006 (2006).
- [62] Eric Thrane¹ and Joseph D. Romano, Phys. Rev. D **88**, 124032 (2013).
- [63] Yves Brihaye and Jutta Kunz Phys. Rev. D **48**, 3884 (1993).
- [64] Sylvie Braibant, Yves Brihaye, Jutta Kunz, Int.J.Mod.Phys. A **8**, 5563-5574 (1993).
- [65] Ruiyu Zhou, Ligong Bian, and Huai-Ke Guo, Phys. Rev. D **101**, 091903(R) (2020).
- [66] K. Funakubo and E. Senaha, Phys. Rev. D **79**, 115024 (2009).
- [67] M. Dvornikov and V. B. Semikoz, Phys. Rev. D **87**, 025023 (2013).
- [68] T. M. Gould and I. Z. Rothstein, Phys. Rev. D **48**, 5917 (1993).
- [69] Rishav Roshan, Graham White, Rev. Mod. Phys. **97**, 015001 (2025).